The Osmotic Migration of Cells in a Solute Gradient

Marc Jaeger,* Muriel Carin,* Marc Medale,* and Gretar Tryggvason#
*Institut Universitaire des Systèmes Thermiques Industriels—Centre National de la Recherche Scientifique UMR 6595, Université de Provence, 13453 Marseille Cedex 13, France, and #Department of Mechanical Engineering, University of Michigan, Ann Arbor, MI 48109-2121 USA

ABSTRACT The effect of a nonuniform solute concentration on the osmotic transport of water through the boundaries of a simple model cell is investigated. A system of two ordinary differential equations is derived for the motion of a single cell in the limit of a fast solute diffusion, and an analytic solution is obtained for one special case. A two-dimensional finite element model has been developed to simulate the more general case (finite diffusion rates, solute gradient induced by a solidification front). It is shown that the cell moves to regions of lower solute concentration due to the uneven flux of water through the cell boundaries. This mechanism has apparently not been discussed previously. The magnitude of this effect is small for red blood cells, the case in which all of the relevant parameters are known. We show, however, that it increases with cell size and membrane permeability, so this effect could be important for larger cells. The finite element model presented should also have other applications in the study of the response of cells to an osmotic stress and for the interaction of cells and solidification fronts. Such investigations are of major relevance for the optimization of cryopreservation processes.

INTRODUCTION

During the freezing of cells in a cryopreservation process, the advance of a solidification front generally leads to a large solute gradient due to the rejection of solute as the water freezes. The purpose of the present paper is to examine the response of cells to a large solute gradient. The main result is that a cell in a solute gradient moves to regions of lower solute concentration due to the uneven flux of water through the cell boundaries. For a cell with internal solute concentration equal to the average concentration outside the cell, water is rejected from the cell on the side facing higher solute distribution, but is absorbed on the side facing lower concentration. If the solute concentration in the cell is not equal to the external average concentration (initial hypertonic or hypotonic environment), the cell initially undergoes a transitional swelling (initial hypotonic environment) or shrinking (initial hypertonic environment) until the cytoplasm achieves an osmotic pressure intermediate between that of the solutions on either side of the cell. The behavior is then the same as in the initial isotonic case.

We investigate the osmotic response of biological cells by examining theoretically and numerically the effect of a solute gradient on a model cell. First, we derive a system of two ordinary differential equations for the cell velocity and the rate at which the cell radius changes. This is done for a cylindrical and a spherical model cell in a constant solute gradient and in the limit when the diffusion of solute is much faster than the osmotic velocity of the cell membrane. We then solve the governing equations numerically using a finite element method with a special front tracking technique to follow the motion of the model cell surface. We study the response of one cell both to a fixed solute gradient and to an advancing solute gradient. Although we account for the cell deformation, we ignore any fluid motion resulting from the reaction of the cell to such deformation, as well as all mechanical aspects of the cell membrane (except the fact that it is permeable for water and impermeable for the solute). The floating or sinking of cells, as reported by Pollard and Leibo (1993) and Pollard et al. (1993), induced by changes in buoyant density as water moves across the membrane is also ignored. This assumption does not put into question our analysis if the concentration gradient is supposed to be directed perpendicular to gravity. In a first approximation, the horizontal osmotic migration can then be assumed to be superposed to the vertical movement of sinking or floating.

Computations with several cells in front of an advancing solidification front show that the osmotic velocity of a row of cells oriented perpendicular to the concentration gradient is higher than for a single cell. The stability of the row is examined by perturbing the cells slightly, but, because the cell velocities are much smaller than the velocity of the solidification front, the cell positions do not change much as the solidification front approaches.

The motivation to study the response of cells to changes in solute concentration comes in large part from cryopreservation. During the freezing and thawing of cells, changes in solute concentration usually lead to osmotic flow of water and cryoprotectants in and out of the cell, and the resulting chemical imbalance and the change in thermodynamic properties has a major impact on the success of the cryopreservation. The survival of cells depends strongly on the cooling rate, and it is found that intermediate cooling rates result in the highest cell survival but cell survival is low at both high and low cooling rates. At high cooling rates, the cell death

Received for publication 8 February 1999 and in final form 21 June 1999.
Address reprint requests to Dr. Marc Jaeger, Technopole de chateau-Gombert, IUSTI-CNRS, 5 rue Enrico Fermi, 13453 Marseille Cedex 13, France. Tel.: +33-4-91-106868; Fax: +33-4-91-106969; E-mail: marc@iusti.univ-mrs.fr.

0006-3495/99/09/1257/11 $2.00

is believed to be due to the formation of ice in the cells. The cell death at low cooling rates has traditionally been attributed to the dehydration of cells resulting from osmotic flow of water out of the cells to match the increase in solute concentration due to solute rejection at a solidification front (Lovelock, 1953; Mazur, 1965; Mazur et al., 1972). Recently, however, several authors have suggested that the cell death at low cooling rates may be due to mechanical interactions between the cells and growing ice crystals. To examine these issues, Ishiguro and Rubinsky (1994) conducted experiments in which the interactions of red blood cells with an advancing solidification front in a directional solidification experiment was studied. For cells in physiological saline, they found that the cells were pushed ahead of the solidification front, often resulting in trapping of cells between advancing ice fingers during unstable cellular solidification. The pushing of cells ahead of a solidification front has been seen by other investigators (Bronstein et al., 1981; Körber, 1988; Lipp et al., 1994), and a similar phenomena is well known in metallurgy where solidification fronts can push small particles and bubbles into the nonsolidified region. The explanation, in the case of particles, is believed to be repulsive van der Waals forces. Large bubbles and particles are, however, overtaken by the front because the surface forces also result in the lowering of the solidification temperature and a slow-down in the propagation of the solidification front behind a particle. Away from the particle, the front propagates with the undisturbed velocity, and the cell can therefore be left behind and entrapped into the solid region if the front velocity is high enough. This has been analyzed by Sasikumar et al. (1989), who gave formulas for the critical velocity for a given particle size.

The volumetric shrinkage of cells due to exosmosis during freezing was first described by Mazur (1963) and the mathematical modeling of cell response to osmotic stresses is currently an active research area. Walcerz (1995) summarized earlier work and presented a computer program to simulate the response of a cell to changes in the external solute concentration and temperature using a well mixed two-chamber model. Batycky et al. (1997) accounted for the spatial variation of the solute concentration by solving the governing equations analytically in a spherical symmetric geometry. Although these studies have yielded major insight into the osmotic transport in and out of cells, they have not addressed the effect of variable solute concentration studied here. In addition to examining the response of a cell to a solute gradient, the present paper introduces a new method that appears to be particularly well suited to study the motion of biological cells and their response to a changing environment. Although we consider only a very simple model here (ignoring all fluid motion and assuming a particularly simple cell structure), the basic method has been used for fluid flow problems, and we expect that extending it to more complex cell problems will not prove to be too difficult. The simplifying assumptions of Walcerz (1995) and Batycky et al. (1997), for example, could then be relaxed.

The paper is organized as follows. We first give the mathematical formulation of the problem specifying all underlying assumptions. The analytical and finite element models are described in the subsequent two sections. The next section presents the results and an analysis of the osmotic migration phenomenon, followed by discussion and conclusions.

FORMULATION

Underlying assumptions

In general, the cell and the ambient fluid are moving and we must solve for both the fluid motion and the distribution of the solute concentration. The solute is advected by the fluid flow, and the solute can influence the fluid motion through change in buoyant density as well as surface tension. Surface tension effects could be considerable, but are difficult to determine because nothing is known about the key parameters—the change with concentration of the interfacial free energy between the solution and the cell surface. The mechanical behavior of the cell (membrane and internal structure) may also modify its motion. However, the mechanical properties of the membrane and the effect of the solute on the membrane properties are not well understood (see, for example, Evans and Parsegian, 1983). The temperature in the fluid and the cell can also vary.

The simplest mathematical description of the response of a cell to varying solute concentration in the ambient fluid is to assume that the fluid motion remains zero and to ignore all mechanical properties of the cell membrane. For a single cell in a fluid with an initially uniform solute distribution, Batycky et al. (1997) showed that fluid velocity is indeed zero while the cell changes volume due to osmotic flow of water through its boundaries. For nonuniform and time-dependent concentration, this may not always be the case. Because the interior ultrastructure of the cells makes relatively little difference to osmotic in and outflow (provided that transport through cytoplasm is much faster then through the plasma membrane), the cells can be modeled as vesicles filled with homogeneous medium. We have studied the influence of the organelles on the osmotic response of the cell by taking into account in the analytical model a nonosmotically active volume distributed uniformly in the cell.

To summarize, the underlying assumptions are: the cells are modeled as simple vesicles, the intracellular and extracellular medium is a binary solution (with parameters chosen to approximate aqueous NaCl solution), the solute is completely nonpermeating, the temperature is constant, the membrane has constant properties, no fluid motion is induced by membrane forces or density variations, and no cell motion is induced by gravity. We further assume no anisotropic forces due to variations in surface free energies with concentration. Additional assumptions specific to the ana-

lytical model or the finite element model are introduced as those are presented.

Mathematical formulation

If we assume zero fluid motion and a dilute solute concentration, then the solute concentration, c_i, both inside and outside the cell is governed by a simple diffusion equation,

$$\frac{\partial c_i}{\partial t} = \nabla \cdot D_i \nabla c_i. \tag{1}$$

Here, D_i is the diffusion coefficient with $i = c$ for the cell and $i = f$ for the surrounding fluid. The cell membrane is impermeable to the solute, but water permeates through the membrane at a normal velocity u_w. The membrane must therefore move with equal and opposite velocity u_n, giving the boundary conditions for the solute at the cell boundary,

$$D_i \frac{\partial c_i}{\partial n} = -c_i u_n. \tag{2}$$

Here n defines the normal vector to the membrane directed toward the external medium. The relative velocity of the membrane with respect to the fluid is directly proportional to the difference in the solute concentration on the cell side of the membrane, c_c, and on the fluid side, c_f,

$$u_n = -u_w = -L(\Pi_f - \Pi_c) \approx -LRT(c_f - c_c). \tag{3}$$

Here, T is the absolute temperature, R is the universal gas constant and L is the hydraulic permeability of the membrane. Π_i is the osmotic pressure in the medium i. In a homogeneous external medium, Eq. 3 leads to the shrinking of cells for hypertonic environment ($u_n < 0$) and to the swelling of cells in the hypotonic case ($u_n > 0$).

These equations can be made nondimensional by assuming a reference size of the cell, r_0, a reference concentration difference Δc, and defining a reference velocity by

$$U = LRT\Delta c. \tag{4}$$

This results in a nondimensional Peclet number, defined by

$$\mathrm{Pe} = \frac{r_0 U}{D_i}, \tag{5}$$

in addition to the ratio of the diffusivities D_c/D_f and the nondimensional initial cell and fluid solute concentrations.

ANALYTICAL MODEL

To obtain an elementary understanding of the behavior of a cell in a nonuniform concentration field, we shall start by examining a simple limiting case of one cell placed in an infinite domain with a uniform concentration gradient aligned with the x-axis. Moreover, we assume that diffusion is much faster than the motion of the cell, so that we may set $\mathrm{Pe} = 0$. The concentration inside the cell is then uniform and the external concentration gradient is determined by a solution of the Laplace equation with zero normal gradient at the cell boundary and a constant gradient far from the cells. The situation is depicted in Fig. 1, where we show a contour plot of the concentration gradient and a cross section through the middle of the cell.

Spherical cell

For a three-dimensional (3D) cell, the solute concentration in the fluid is given by the solution of Laplace's equation with zero normal gradient at the cell boundary (Lamb, 1932),

$$c_f(\theta) = c_f^0 - Gx_c - \tfrac{3}{2} Gr\cos\theta, \tag{6}$$

where the angle θ is defined in Fig. 1, r is the radius of the cell, c_f^0 is the concentration in the fluid at $x = 0$ and x_c is the location of the cell centroid. G is the solute gradient far from the cell. The normal velocity of the cell membrane is therefore dependent on the angle,

$$u_n(\theta) = -LRT(c_f^0 - Gx_c - \tfrac{3}{2} Gr\cos\theta - c_c). \tag{7}$$

The rate of change of the volume V of the cell is found by integrating the normal velocity over the cell boundary,

$$\begin{aligned}\frac{dV}{dt} = \oint_S u_n\, ds &= -LRT\int_0^{2\pi}\int_0^{\pi}(c_f^0 - Gx_c \\ &\quad - \tfrac{3}{2} Gr\cos\theta - c_c) r^2 \sin\theta\, d\theta\, d\varphi \\ &= -4\pi LRTr^2(c_f^0 - Gx_c - c_c).\end{aligned} \tag{8}$$

Here, S is the cell boundary and the first two terms in the parentheses ($c_f^0 - Gx_c$) are the undisturbed solute concentration at the cell centroid. For a spherical cell, $V = \tfrac{4}{3}\pi r^3$, and the total amount of solute inside the cell is constant, so that $r^3 c_c = r_0^3 c_c^0$, where c_c^0 is the cell concentration at zero time and r_0 is the initial radius. This can be rewritten as an evolution equation for the radius of the cell,

$$\frac{dr}{dt} = -LRT\left(c_f^0 - Gx_c - c_c^0\left(\frac{r_0^3}{r^3}\right)\right). \tag{9}$$

The velocity of the cell centroid is given by

$$\frac{dx_c}{dt} = \frac{d}{dt}\left(\frac{1}{V}\int_{CV} x\, dv\right) = \frac{1}{V}\frac{d}{dt}\int_{CV} x\, dv - \frac{x_c}{V}\frac{dV}{dt}, \tag{10}$$

where CV indicates that the integration is over the cell volume. Using that,

$$\frac{d}{dt}\int_{CV} x\, dv = \oint_S x u_n\, ds, \tag{11}$$

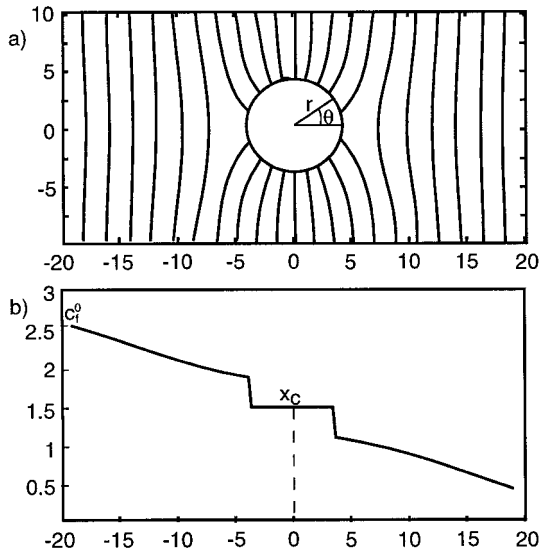

FIGURE 1 Schematic. (*a*) Concentration contour plot and (*b*) cross section through the middle of the cell in the limit of very fast diffusion (Pe = 0).

and $x = x_c + r\cos\theta$, we find that

$$\frac{dx_c}{dt} = \frac{1}{V}\oint_S xu_n\,ds - \frac{x_c}{V}\frac{dV}{dt}$$

$$= \frac{1}{V}\oint_S r\cos\theta u_n\,ds + \frac{x_c}{V}\frac{dV}{dt} - \frac{x_c}{V}\frac{dV}{dt}$$

$$= \frac{r^3}{V}\int_0^{2\pi}\int_0^{\pi} u_n\cos\theta\sin\theta\,d\theta\,d\varphi. \qquad (12)$$

Substituting for the normal velocity and carrying out the integration yields

$$\frac{dx_c}{dt} = \frac{3}{2}LRTGr. \qquad (13)$$

We note that the velocity of the centroid depends only on the gradient of the solute concentration and not on the absolute value. The rate of change of volume of the cell does, in contrast, depend on the absolute value, and the cell velocity increases with volume.

These equations can be made nondimensional by the reference velocity defined above, the initial cell radius, and the fluid concentration gradient times the initial cell radius ($\Delta c = Gr_o$). Denoting the nondimensional variables by a tilde ($\tilde{r} = r/r_0$, $\tilde{t} = LRTGt$ and $\tilde{c} = c/Gr_0$), we have

$$\frac{d\tilde{x}_c}{d\tilde{t}} = \frac{3}{2}\tilde{r}, \qquad (14)$$

$$\frac{d\tilde{r}}{d\tilde{t}} = -\left(\tilde{c}_f^0 - \tilde{x}_c - \tilde{c}_c^0\left(\frac{1}{\tilde{r}^3}\right)\right),$$

where $\tilde{c}_f^0$ is the undisturbed fluid concentration at $x = 0$ divided by Gr_o and $\tilde{c}_c^0$ is the cell solute concentration at time zero, nondimensionalized in the same way. The initial nondimensional radius is 1, and the initial cell position can be taken to be 0. It is perhaps a little counterintuitive that both the initial cell concentration and the undisturbed concentration at the initial position must be given, rather than simply the initial difference. The fact that the solution depends on the absolute value of the cell concentration can be seen by considering the special case when the cell concentration is zero. Then it remains zero for all time, whereas any finite value will increase as the cell becomes smaller. If the initial cell concentration is zero, the equations become linear and can be solved to give

$$x(t) = \tilde{c}_f^0\left(1 - \cosh\sqrt{\frac{3}{2}}t\right) + \sqrt{\frac{3}{2}}\sinh\sqrt{\frac{3}{2}}t, \qquad (15)$$

$$r(t) = -\sqrt{\frac{2}{3}}\tilde{c}_f^0\sinh\sqrt{\frac{3}{2}}t + \cosh\sqrt{\frac{3}{2}}t.$$

The cell radius becomes zero at $t = \sqrt{2/3}\tanh^{-1}(\sqrt{3/2}/\tilde{c}_f^0)$ and the cell only moves a short distance. We note that this case, where the initial intracellular concentration is zero, is biologically unimportant.

Cylindrical cell

For a two-dimensional (2D) cell, the solute concentration is given by (Lamb, 1932)

$$c_f(\theta) = c_f^0 - Gx_c - 2Gr\cos\theta, \qquad (16)$$

and a similar analysis as above yields

$$\frac{dx_c}{dt} = 2LRTGr, \qquad (17)$$

$$\frac{dr}{dt} = -LRT\left(c_f^0 - Gx_c - c_c^0\left(\frac{r_0^2}{r^2}\right)\right).$$

Using the same reference quantities as before, we obtain the following nondimensional equations,

$$\frac{d\tilde{x}_c}{d\tilde{t}} = 2\tilde{r}, \qquad (18)$$

$$\frac{d\tilde{r}}{d\tilde{t}} = -\left(\tilde{c}_f^0 - \tilde{x}_c - \tilde{c}_c^0\left(\frac{1}{\tilde{r}^2}\right)\right).$$

The cell velocity is slightly higher than what we found for the 3D cell, but the structure of the equations is the same.

Spherical cell with a nonosmotically active volume V_b

In general, a finite nonosmotically active volume V_b, that takes into account organelles and molecules of water that

are osmotically inactive, exists within the cell (Savitz et al., 1964). The intracellular concentration is then given by

$$c_c = \frac{\text{moles of salt}}{\text{osmotically active volume}} = \frac{N}{V - V_b}. \quad (19)$$

Because the number of salt moles is constant, the concentration within the cell is

$$c_c = c_c^0 \frac{V_0 - V_b}{V - V_b}, \quad (20)$$

where V_0 is the initial cell volume. With $V_b = \alpha V_0 (0 < \alpha < 1)$, the cell concentration can be rewritten as

$$c_c = c_c^0 \frac{V_0(1 - \alpha)}{V - \alpha V_0} = c_c^0 \frac{r_0^3(1 - \alpha)}{r^3 - \alpha r_0^3}. \quad (21)$$

The rate of change of the cell radius is then

$$\frac{dr}{dt} = -LRT\left(c_f^0 - Gx_c - c_c^0\left(\frac{1 - \alpha}{(r^3/r_0^3) - \alpha}\right)\right). \quad (22)$$

The velocity of the cell centroid is the same as found for a 3D cell without a nonosmotically active volume, because the velocity does not depend on the cell concentration.

The nondimensional equations for a spherical cell with a nonosmotically active volume are

$$\frac{d\tilde{x}_c}{d\tilde{t}} = \frac{3}{2}\tilde{r}, \quad (23)$$

$$\frac{d\tilde{r}}{d\tilde{t}} = -\left(\tilde{c}_f^0 - \tilde{x}_c - \tilde{c}_c^0 \frac{1 - \alpha}{\tilde{r}^3 - \alpha}\right).$$

FINITE ELEMENT MODEL

To simulate more general situations, we have developed a 2D numerical model based on the finite element method complemented with a special interface tracking algorithm. Indeed, the numerical solution of the equations governing the motion of cells in a concentration gradient are made difficult by the presence of moving cell boundaries, at which there is a discontinuity in the solute concentration. To overcome this problem, we use a specially designed finite element method. The method is an extension of the one described by Medale and Jaeger (1997) and Lock et al. (1998). Although the original method was developed for problems with fluid flow, here we have used it only for the diffusion of the solute concentration.

To solve the diffusion equation, we use a three-node triangular element with a piece-wise linear approximation for the solute concentration and an implicit time integration method. The integral form associated with the variational statement of diffusion of solute concentration is

$$W_c = \int_\Omega \left[\delta c \frac{\partial c_i}{\partial t} + D_i \nabla(\delta c) \cdot \nabla c_i\right] d\Omega + \int_S \delta c c_i u_n \, dl, \quad (24)$$

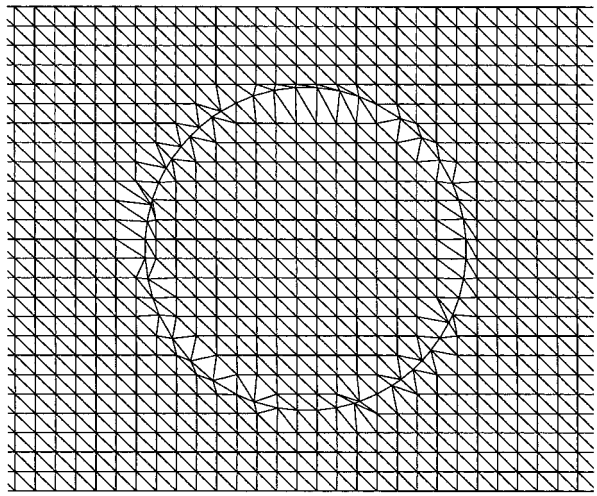

FIGURE 2 Finite element mesh in the cell region.

where $i = c$ or $i = f$. δc is the weighting function associated with the solute, and we have used Eq. 2 for the boundary fluxes. The solute distribution in the fluid and the cell is found on a stationary mesh, which is locally adapted at each time step in such a way that element boundaries align with the membrane. The mesh adaptation used here differs from that which we used in Lock et al. (1998). Instead of cutting the elements crossed by an interface, here the mesh fitting is obtained by moving the nodes aligned with the membrane (see Fig. 2). This model differs from an Arbitrary Lagrangian Eulerian formulation because the nodes located on the membrane can change from one time step to the other and the motion of the mesh is limited to the nodes on the membrane.

The aim of the mesh adaptation is both to give an accurate numerical description of the discontinuity in material properties between the inside and the outside of a cell and, most importantly, to allow us to model accurately the water flux through the membrane by applying the boundary condition (Eq. 2) to the elements next to the membrane. To take into account the solute concentration discontinuity inducing this water flux, we replace each node on the interface by two nodes, one for the cell fluid and another for the surrounding fluid. Once the mesh has been adapted to the membrane position, the value of the solute at the next time step is computed. This computation yields new values of the discontinuity in solute concentration at the membrane and thus new values of the osmotic velocity (Eq. 3). The membrane mesh is then moved Lagrangially. In addition to its accuracy, this approach allows us easily to take into account the mechanical behavior of the membrane (stress–strain analysis). For that purpose, we would have to complement the solute diffusion model presented here with a mechanical one. This will be done in a future work. In the present study, we have only considered two extreme cases: the membrane can deform freely or cannot deform at all, as assumed in the analytical analysis. In the first case, the nodes of the membrane mesh are simply moved in the normal direction with

a magnitude given by the osmotic velocity. In the second case, this step is followed by a repositioning of the nodes uniformly on a circle with the same centroid and the same area as the cell after the transport step.

RESULTS

One cell in a constant solute concentration gradient

We have solved Eqs. 14, 18, and 23 numerically (using Mathematica) for a few different initial conditions (c_c^0 = 0.5, 1.0, and 1.5 times c_f^0). In Fig. 3, we have plotted (in nondimensional variables) the evolution of the cell radius and the cell centroid, obtained with Eq. 18, versus time for the three different initial cell solute concentrations. This figure shows that, if the cell solute concentration is initially equal to the concentration of the fluid (initial isotonic environment, $c_c^0 = c_f^0$), water flows out of the cell on the left side where the outside concentration is higher than inside the cell, and into the cell on the right where the cell concentration is higher. The cell, therefore, moves to the right toward a lower ambient solute concentration. As the cell moves, the inflow of water increases because the concentration jump on the right becomes larger. This increases the size of the cell and reduces the cell solute concentration, thus equilibrating the in- and the outflow. Since the velocity of the cell is proportional to its radius, the velocity increases slightly as it moves to lower concentrations. If the initial cell concentration differs from the average concentration in the fluid, the evolution of the cell exhibits two steps: 1) a rapid shrinking or swelling of the cell to achieve a concentration intermediate between those of the solution on either side, and 2) migration of the cell toward lower concentration regions in the same manner as in the initial isotonic case. During the first stage, the water flux is outward or inward over all the area, although larger on the side of higher concentration jump. Thus, the cell centroid must remain within the space initially occupied by the cell. However, once the cell concentration becomes intermediate between the high- and low-concentration sides, there is a net flux through the cell, and so, substantial displacement is possible. As a result, the migration velocity is a strong function of the amount of solute initially in the cell, in addition to depending on the solute gradient in the fluid. If $c_c^0 = 1.5\ c_f^0$, the cell first swells before migrating and thus reaches a higher velocity. On the contrary, if $c_c^0 = 0.5\ c_f^0$, the cell first shrinks, leading to a lower velocity. Similar plots for Eqs. 14 and 23 (not shown) exhibit the same behavior but with different asymptotic cell velocities.

What is the nature of the force causing the cell to move? One way of looking at it is to consider the relative motion of solutes and solvent. Solutes diffuse from high concentration to low concentration. Incompressibility requires that, at the same time, an equal volume of solvent moves from low solute concentration to high solute concentration. This flux is more easily understood as solvent moving from high solvent concentration to low solvent concentration. The solutes inside the cell also diffuse from high (solute) concentration to low, but, due to the semipermeability of the cell membrane, they are constrained to remain inside. The cell membrane and other ultrastructural components therefore travel with the solutes. The water, in contrast, can permeate the membrane, so there is a flux of water through the cell in a direction opposite to the motion of the cell. The force that acts on the membrane and moves the cell is the difference in osmotic pressure acting on either side of it. Consider a cell in a gradient of concentration decreasing to the right at a time when the intracellular solution has already achieved a concentration intermediate between that of the solution to its right and its left. Water moves in the cytoplasm much more rapidly than it does in through the membrane, so the solute concentration inside the cell is nearly uniform. On the left side of the cell, the osmotic pressure is greater outside than inside the cell and so exerts a force to the right. On the right side of the cell, the osmotic pressure is greater inside than outside the cell and so also exerts a force to the right. The total force is therefore to the right (see Fig. 4). At a molecular and Newtonian level, we may ask why the force on the membrane exerted by the solutes, which move to the right in our example, is greater than that exerted by the equal volume of solvent. This is simply due

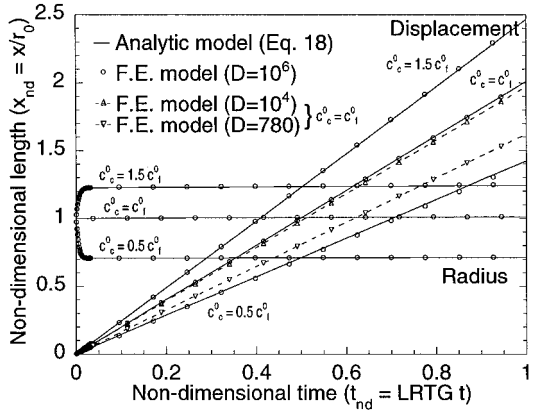

FIGURE 3 Evolution of the cell radius and the cell centroid for different initial cell concentrations (c_c^0 = 0.5, 1.0, and 1.5 times c_f^0, with c_f^0 = 93.6).

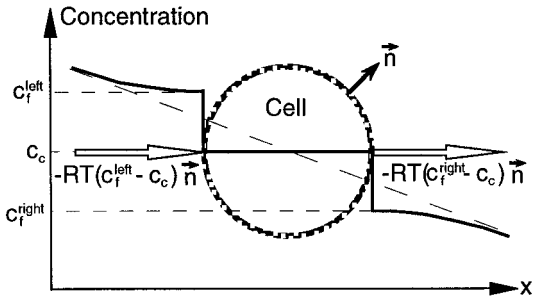

FIGURE 4 Schematic. Osmotic pressure acting on a cell placed in a constant concentration gradient (c_f^{left} and c_f^{right} are the concentration in the fluid on the left and right sides of the cell).

to the semipermeability. Overall, the water molecules that pass through the membrane have little change in momentum and therefore exert relatively little force on the membrane, whereas the solute molecules all recoil from the membrane and therefore suffer a large momentum change and thus exert a larger force on membrane.

The importance of osmotic migration can be estimated by considering realistic values for the various parameters in the expression for the cell velocity. Wollhöver et al. (1985) show a few examples of solute rejection in front of a solidification interface. Their data suggest that gradients of the order of 0.01 M/μm are not uncommon. The permeability of erythrocytes is in the range of 5–10 μm/min·atm, i.e., around 10^{-12} m/s·Pa (Aggarwal et al., 1988; Gilmore et al., 1995), and Körber (1988) finds a mean radius of 4.5 μm for this type of cells. We compare, in Table 1, the velocities obtained with the three different sets of Eqs. 14, 18, and 23 using $L = 10$ μm/min·atm ($1.66\ 10^{-12}$ m/s·Pa), the freezing temperature of water ($T = 273$ K), R = 0.08206 atm/M·K, and a cell radius of 5 μm. We find that the expression for the cell velocity in the zero Peclet number limit gives values around 0.2 μm/s.

Table 1 shows that the correction introduced to take into account the nonosmotically active volume yields a difference of less than 5%. The 2D model (Eq. 18) overestimates the cell velocity by about 30% in comparison with the 3D model (Eq. 14). However the similarity of the results for the 2D and 3D calculations justify restricting a detailed analysis to 2D calculations. Because of the greatly reduced number of nodes in a 2D calculation, it is therefore possible to increase the spatial resolution and/or the complexity of the system analyzed.

To test the finite element model, we have simulated the behavior of a cylindrical cell in a constant solute concentration gradient. Our computed response can then be compared to the 2D analytical solution (Eq. 18). The computational domain is a 2D rectangle that is 100×50 μm. The solute concentration is specified along the left and the right boundaries, and a zero flux condition is imposed along the top and the bottom ones. A cylindrical cell (with initial radius $r_0 = 5$ μm) is placed at the center of the domain and we follow its motion as it moves to the right. The finite element mesh consists of 4800 three-node triangles and is refined in the center of the domain where the cell is (see Fig. 2). The membrane mesh consists of 120 two-node linear elements. The computation, which is done in dimensional variables, uses the physical parameters (r_0, L, R, T, c_c^0 and c_f^0) mentioned above, and we have assumed that the diffusion coefficients in the cell and the ambient fluid are equal. Three different values ($D = 10^6$, 10^4, and 780 μm^2/s) have been considered to study the influence of the Peclet number on the osmotic response of the cell. The last diffusivity corresponds to a published value for diffusion of salt in water (Wollhöver et al., 1985). The comparison with the analytical model can be found in Fig. 3, where the solid line shows the analytical results and the markers represent the numerical ones. For clarity, the influence of the Peclet number on the results is illustrated in Fig. 3 only for the case $\tilde{c}_c^0 = \tilde{c}_f^0$. It is clear that, as the Peclet number becomes smaller, the results approach the analytical prediction. Beyond $D = 10^6$ μm^2/s no difference can be seen between the analytical and the numerical solutions. In Fig. 5, we show the solute concentration in a cross section through the middle of the cell for the lowest and the highest values of the diffusivity ($D = 780$ μm^2/s, $D = 10^6$ μm^2/s) at the same time step. As the cell moves, it is clear that it disturbs the solute gradient, whereas the solute concentration behind the cell is reduced due to the flow of pure water from the cell, solute piles up in front of the cell where water moving into the cell leaves the solute behind. A moving cell at a finite Peclet number therefore experiences a smaller jump in ambient solute concentration than does a cell at Pe = 0. Although this should slow the cell down, the finite Peclet number also results in a nonuniform distribution inside the cell, and the reduction in the velocity is not as large as if the inside concentration remained uniform.

The computations have been done allowing the membrane to deform freely as well as keeping it circular (node repositioning). No difference is observed on the result. This is as expected because the flux is proportional to cos θ for a single cell in a linear concentration gradient. The only difference is observed in the structure of the membrane

TABLE 1 Comparison of asymptotic cell velocity obtained with the three versions of the analytical model (2D, 3D, and 3D taking into account the nonosmotically active volume with $\alpha = 0.2$).

	$c_c^0 = 0.5\ c_f^0$	$c_c^0 = c_f^0$	$c_c^0 = 1.5\ c_f^0$
2D	0.268 μm/s	0.382 μm/s	0.470 μm/s
3D ($\alpha = 0$)	0.225 μm/s	0.284 μm/s	0.325 μm/s
3D ($\alpha = 0.2$)	0.237 μm/s	0.282 μm/s	0.316 μm/s

The results have been obtained with the following dimensional values: $r_0 = 5$ μm, $G = 0.01$ M/μm, $L = 10$ μm/min·atm (1.66×10^{-12} m/s·Pa), $T = 273$ K, and for three initial cell concentrations: $c_c^0 = 0.5$, 1.0, and 1.5 times c_f^0.

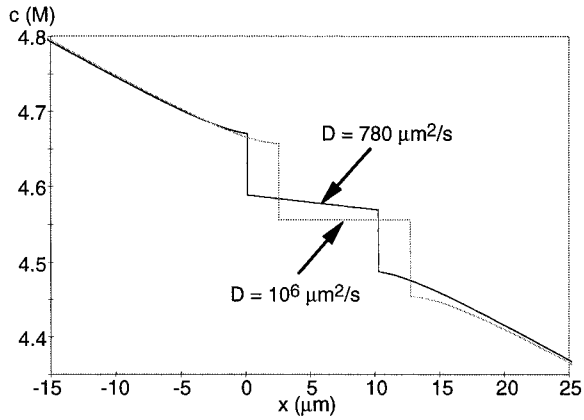

FIGURE 5 Influence of the diffusion coefficient on the concentration profile near the cell (cross section through the middle of the cell) at the same time step.

mesh. As the cell moves to the right, the nodes, which are uniformly distributed in the beginning, move along the membrane toward the left side of the cell. To continue the computations for a long time, it would thus be necessary to add new nodes at the front and delete old ones at the back.

One cell in front of an advancing ice front

The solute concentration in front of an advancing solidification front increases as the solute is rejected by the solidified region. The magnitude of the resulting solute concentration gradient depends on the front velocity, which is a function of the cooling rate. Examples of concentration profiles in front of an advancing planar ice front can be found in O'Callaghan et al. (1980) and Wollhöver et al. (1985). Given a front velocity and assuming that the solid phase rejects all the solute, our finite element model is able to predict such profiles. Indeed, as the front moves, the solute concentration in the liquid phase is governed by Eq. 1 with boundary condition Eq. 2, so the solid–liquid interface can be simulated in the same way as a cell membrane, but with a specified velocity instead of Eq. 3. The solute concentration on the other side of the front is set equal to zero. Figure 6, where the evolution of the salt concentration ahead of a planar ice front advancing at a velocity of 1 μm/s is shown, illustrates this capability of the model. Initially, the solute concentration in the liquid phase is a constant value of 0.145 M. This corresponds to a hypotonic solution in which the red blood cells take a spherical shape. We are now in a position to consider more realistic situations than those presented in the previous section and study the osmotic response of one or more cylindrical cells in front of an advancing solidification front.

In Fig. 7, we plot (in dimensional variables) the evolution of the cell volume and the cell centroid versus time for three different values of the speed of the solidification front. The conditions here are almost the same as in the previous simulations in terms of grid refinement, time step, and top and bottom boundary conditions. The type of cell considered is also the same: a spherical cell with an initial radius of 5 μm and membrane properties as specified in the previous section. To have a sufficiently long time to study the cell response before the solidification front reaches the cell, the left boundary has been placed at 100 μm from the cell region. At this boundary, the solute concentration is zero (because it is inside the solid phase). The right boundary is also 100 μm from the initial position of the cell. On this side, we prescribe the concentration values that would exist at this point if there was no cell in the domain. This value is obtained by a separate computation, like the one presented on Fig. 6, and evolves as the solidification front advances. Initially, the concentration in the liquid phase and inside the cell is equal to 0.145 M. Figure 7 shows clearly the influence of the front velocity on the osmotic response. The increased rate of shrinkage with increasing solidification velocity corresponds well to published results (Silvarès et al., 1975). For the parameters simulated here, the cell speed induced by the osmotic flow is about 1% of the front velocity (0.15 μm/s for V_{ice} = 10 μm/s, 0.02 μm/s for V_{ice} = 2 μm/s, and 0.01 μm/s for V_{ice} = 1 μm/s).

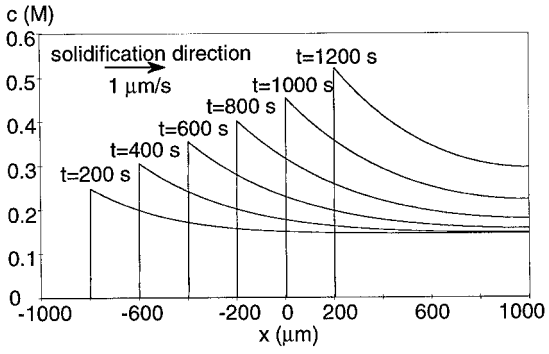

FIGURE 6 Profile of salt concentration ahead of a planar ice front advancing at a velocity of 1 μm/s at different time steps.

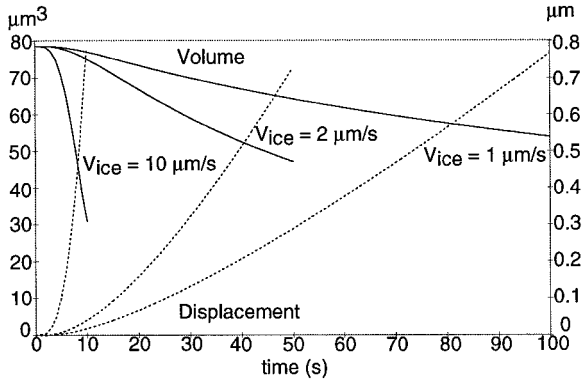

FIGURE 7 Evolution of the cell volume (*solid lines*) and cell centroid (*dotted lines*) versus time for three different speeds (V_{ice}) of the solidification front.

Many cells in front of an advancing ice front

Although the solidification front will frequently encounter one cell at a time, after a long time (or if the cell concentration is high) it is possible that several cells pile up in front of it. Such accumulation is seen, for example, in some of the figures in Ishiguro and Rubinsky (1994). To examine the effect of a solute concentration gradient on several cells, we have done simulations with a row of identical cells parallel to the ice front. The conditions of these computations are the same as for the single cell case with a front velocity of 1 μm/s. We have studied the influence of the separation between the cells by considering increasing initial gap values (0.2, 1, and 6 times r_0). The evolution of the cell volume and the cell centroid versus time for the different cases are compared on Fig. 8. The results obtained for the single cell case are also shown. The cell velocity becomes larger as the gap between the cells decreases. The influence on the cell volume is not as pronounced, although it is reduced a little

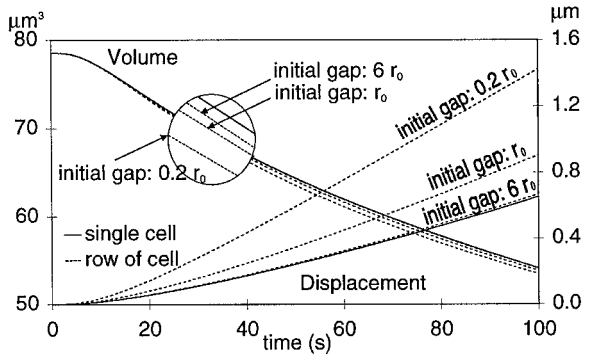

FIGURE 8 Evolution of the cell volumes and the cell centroids versus time for a row of cells ahead of an ice front advancing at 1 μm/s, along with the single cell case.

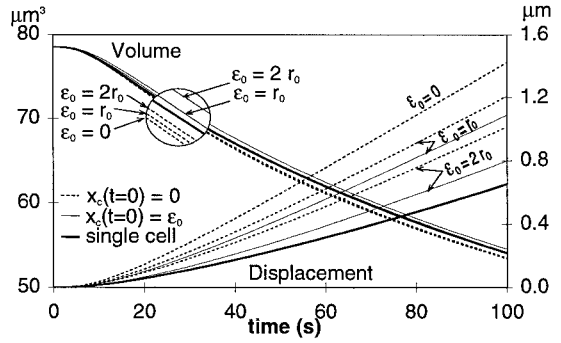

FIGURE 10 Evolution of the cell volume and the cell centroid displacement $[x_c - x_c\,(t = 0)]$ versus time for a row of cells separated by a gap of $0.2r_0$ and initially perturbed by moving horizontally every three cells a small distance ϵ_o to the right along with the nonperturbed case ($\epsilon_o = 0$) and the single cell case.

faster when the cells are closer. To explain this phenomenon, Fig. 9 shows the solute concentration profile at different times in a cross section through the middle of one cell, for an initial gap between the cells of 0.2 r_0, along with the profiles obtained for the single-cell case. The solute concentration between the solidification front and the cells reaches a higher value for a row of cells due to the blockage that the cells provide for the diffusion of solute downstream. Thus, the drop in concentration across the cells is considerably larger and the cells move faster.

To see if osmotic migration can explain, at least in part, the alignment of cells in front of a solidification front, we have done additional computation, where a row of cells separated by a gap of 0.2 r_0 is perturbed initially by moving every third cell a small distance ϵ_o to the right. Two initial perturbations have been examined: $\epsilon_o = r_0$ and $\epsilon_o = 2r_0$. The cell volume and the cell centroid are plotted versus time in Fig. 10, along with the non-perturbed case and the single cell case. The figure shows that the velocities of the more perturbed cells are lower than for the unperturbed one, because the blocking is smaller, and that the difference between the velocities of the cells moved to the right and the cells left in place increases with the magnitude of the perturbation. Therefore, it is likely that the cells left behind would eventually catch up and the cells become perfectly aligned. The motion is, however, very slow and the solidification front reaches the cells before they have time to do so.

Finally, we have done one computation to illustrate the interaction between cells when they are very close. For that purpose, we have considered a group of three cells aligned with the solidification front. Initially there is no vertical gap between the cells, and the middle cell is moved a distance r_0 to the right (i.e., toward the more dilute solution). Unlike our previous computations, here, we obtain a nonnegligible deformation if we let the cell membrane deform freely. This is illustrated in Fig. 11, where we have plotted the contours of the solute concentration in the cell region just before the solidification front reaches the cells. The deformation of the middle cell is largest because of the influence of the two surrounding cells. Although the deformation could have an impact on the cell itself, or on aspects of the problem not

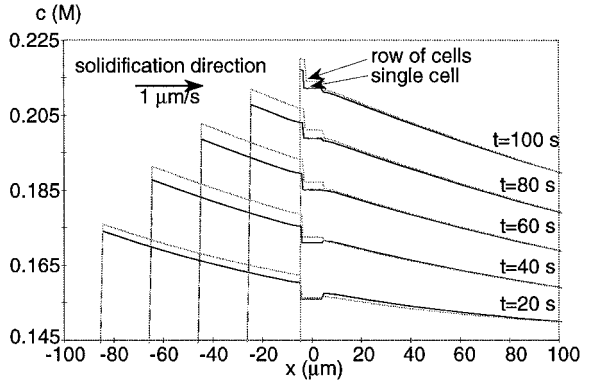

FIGURE 9 The solute concentration profile at different time steps in a cross section through the middle of one cell for an initial gap of $0.2r_0$ between the cells and for the single cell case.

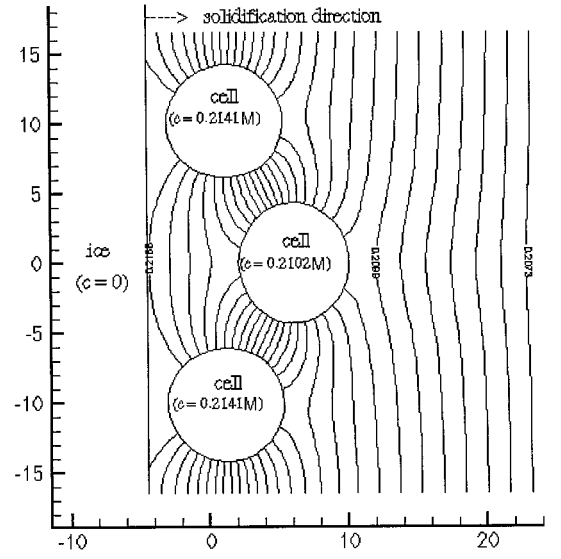

FIGURE 11 Concentration contour plot just before the ice front reaches a group of three cells initially very close together.

taken into account in this study, it has only a small influence on the evolution of the cell volume and the cell velocity.

DISCUSSION AND CONCLUSION

We are not aware of any previous discussion of the motion of cells induced by a solute concentration gradient. It is not mentioned, for example, by Körber (1988) in his review article nor by Batycky et al. (1997), who suggest nonuniform solute concentrations as one extension of their investigation. Although our results are based on simplifying assumptions about the nature of the cells, they show that osmotic migration takes place as soon as a solute concentration gradient occurs, as in the presence of an advancing solidification front. Although the theory and simulations predict rather small velocities for the cells considered here, the effect could be much more important for cells with higher permeability and/or size.

In the limit of a Peclet number equal to zero and for a solute concentration gradient of 0.01 M/μm, the analytical model leads to cell velocities around 0.2 μm/s. For a finite Peclet number, the velocity is reduced somewhat, but the order of magnitude remains the same. The finite element computations simulating the osmotic response of a single cell ahead of a moving planar solidification front predict cell velocities of the order of 1–2% of the front speed for cells with permeability and size of erythrocytes. Moreover, the model has shown that the velocity can increase by a factor of two or more when the cells are lined up in a row ahead of the solidification front. The velocities found here can be compared with the critical velocity for human erythrocytes reported by Lipp et al. (1994), which is slightly above 1 μm/s. Although the migration velocities appear to be too small to explain the motion of cells away from a solidification front, the phenomena can possibly be put to a practical use in measurements of cell properties. The hydraulic permeability of cells is usually measured by monitoring volume changes during a change in the ambient solute concentration, but it may be possible to obtain the same information by measuring the motion of a cell in a concentration gradient. Since displacement is measured more easily than volume change, such a technique may have some appeal.

In addition to the analytical formulation of the osmotic migration of cells in a constant gradient, we have developed a 2D finite element model. The excellent agreement between these two models validates the finite element approach. It is clear that it allows us to deal with more complex situations as demonstrated by the study of the action of a moving ice front on one or more cells. Although this preliminary study is based on many simplifying assumptions (2D, constant temperature, a single impermeable solute, constant membrane permeability, effect of intracellular organelles ignored, simplified mechanical behavior of the membrane, and so on), extensions of the model are possible in a wide range of physical phenomena. For example, the effect of cryoprotectant agents (permeable or not to the membrane), which are generally added to the extracellular medium before cooling, could be taken into account. However, future developments will focus first on the extensions of the method to 3D cells and on the introduction of the temperature as an unknown of the problem. The computed results could then be compared to experimental data. The coupling of the thermal equation with diffusion will allow us to study more accurately the interaction of cells with a solidification front because the influence of the cells on the solidification process could then be taken into account. The availability of a sophisticated simulation tool could offer new possibilities for the use of combined measurement/simulations techniques for the determination of the properties of cell membrane. By studying the osmotic response of a cell as a function of its initial orientation, it should be possible to obtain local information for the membrane and to determine the permeability as a function of other parameters such as temperature and solute concentrations.

Funding for this work was provided by the French Ministere de la Defense through DGA Contract 96.1191A and in part by United States National Science Foundation grant CTC-9503208. We wish to thank Dr. G. Novakovitch for discussions during the early stages of the project. G. Tryggvason wishes to thank Institut Universitaire des Systèmes Thermiques Industriels for hosting him for one month in April and May of 1998.

REFERENCES

Aggarwal, S. J., K. R. Diller, and C. R. Baxter. 1988. Hydraulic permeability and activation energy of human keratinocytes at subzero temperature. *Cryobiology.* 25:203–211.

Batycky, R. P., R. Hammerstedt, and D. A. Edwards. 1997. Osmotically driven intracellular transport phenomena. *Phil. Trans. R. Soc. Lond. A.* 355:2459–2488.

Bronstein, V. L., Y. A. Itkin, and G. S. Ishkov. 1981. Rejection and capture of cells by ice crystals in freezing aqueous solutions. *J. Cryst. Growth.* 52:345–349.

Evans, E. A., and V. A. Parsegian. 1983. Energetics of membrane deformation and adhesion in cell and vesicle aggregation. *Ann. N.Y. Acad. Sci.* 416:13–33.

Gilmore, J. A., L. E. McGann, J. Liu, D. Y. Gao, A. T. Peter, F. W. Kleinhans, and J. K. Critser. 1995. Effect of cryoprotectant solutes on water permeability of human spermatozoa. *Biol. Reprod.* 53:985–995.

Ishiguro, H., and B. Rubinsky. 1994. Mechanical interactions between ice crystals and red blood cells during directional solidification. *Cryobiology.* 31:483–500.

Körber, C. 1988. Phenomena at the advancing ice–liquid interface: solutes, particles and biological cells. *Q. Rev. Biophys.* 21:229–298.

Lamb, H. 1932. Hydrodynamics. Cambridge University Press, Cambridge, U.K.

Lipp, G., S. Galow, C. Körber, and G. Rau. 1994. Encapsulation of human erythrocytes by growing ice crystals. *Cryobiology.* 31:305–312.

Lock, N., M. Jaeger, M. Medale, and R. Occelli. 1998. Local mesh adaptation technique for front tracking problems. *Int. J. Numer. Meth. Fluids.* 28:719–736.

Lovelock, J. E. 1953. The hemolysis of human red blood cells by freezing and thawing. *Biochim. Biophys. Acta.* 10:414–426.

Mazur, P. 1963. Kinetics of water loss from cells at subzero temperatures and the likelihood of intracellular freezing. *J. Gen. Physiol.* 47:347–369.

Mazur, P. 1965. Causes of injury in frozen and thawed cells. *Fed. Proc.* 24:175–182.

Mazur, P., S. P. Leibo, and E. H. Chu. 1972. A two-factor hypothesis of freezing injury. Evidence from Chinese hamster tissue-culture cells. *Exp. Cell. Res.* 71:345–355.

Medale, M., and M. Jaeger. 1997. Numerical simulation of incompressible flows with moving interfaces. *Int. J. Numer. Meth. Fluids.* 24:615–638.

O'Callaghan, M. G., E. G. Cravalho, and C. E. Huggins. 1980. Instability of the planar freeze front during solidification of an aqueous binary solution. *J. Heat Transfer.* 102:673–677.

Pollard, J. W., and S. P. Leibo. 1993. Comparative cryobiology of in vitro and in vivo derived bovine embryos. *Theriogenology.* 39:287.

Pollard, J. W., C. Plante, N. Songsasen, and S. P. Leibo. 1993. Correlation of sensitivity to chilling and freezing with buoyant density of mammalian embryos. *Cryobiology.* 30:631.

Sasikumar, R., T. R. Ramamohan, and B. C. Pai. 1989. Critical velocities for particle pushing by moving solidification fronts. *Acta Metallica.* 37:2085–2091.

Savitz, D., V. W. Sidel, and A. K. Solomon. 1964. Osmotic properties of human red cells. *J. Gen. Physiol.* 48:79–94.

Silvarès, O. M., E. G. Cravalho, W. M. Toscano, and C. E. Huggins. 1975. The thermodynamics of water transport from biological cells during freezing. *J. Heat Transfer.* 97:582–588.

Walcerz, D. B. 1995. Cryosim: a user-friendly program for simulating cryopreservation protocols. *Cryobiology.* 32:35–51.

Wollhöver, K., C. Körber, M. W. Scheiwe, and U. Hartmann. 1985. Unidirectional freezing of binary aqueous solutions: an analysis of transient diffusion of heat and mass. *Int. J. Heat Mass Transfer.* 28: 761–769.